molecular pharmaceutics

articles

Ethyl-2-amino-6-bromo-4-(1-cyano-2-ethoxy-2-oxoethyl)-4*H*-chromene-3-carboxylate (HA 14-1), a Prototype Small-Molecule Antagonist against Antiapoptotic Bcl-2 Proteins, Decomposes To Generate Reactive Oxygen Species That Induce Apoptosis

Jignesh M. Doshi,[†] Defeng Tian,[†] and Chengguo Xing*

Department of Medicinal Chemistry, College of Pharmacy, University of Minnesota, 8-101 WDH, 308 Harvard Street SE, Minneapolis, Minnesota 55455

Received June 21, 2007; Revised Manuscript Received August 2, 2007; Accepted August 7, 2007

Abstract: Overexpressing antiapoptotic Bcl-2 proteins to suppress apoptosis is one major mechanism via which cancer cells acquire drug resistance against cancer therapy. Ethyl-2-amino-6-bromo-4-(1-cyano-2-ethoxy-2-oxoethyl)-4*H*-chromene-3-carboxylate (HA 14-1) is one of the earliest small-molecule antagonists against antiapoptotic Bcl-2 proteins. Since its discovery, HA 14-1 has been shown to be able to synergize a variety of anticancer agents. HA 14-1 also could selectively eliminate tumor cells with elevated level of Bcl-2 protein. HA 14-1, therefore, is being intensely investigated as a potential anticancer agent. Previous reports of HA 14-1 implied that it may not be stable, raising the question of whether HA 14-1 is a suitable drug candidate. The potential stability also raised the concern about whether HA 14-1 is the bioactive species. In this report, we confirm that HA 14-1 is not stable under physiological conditions: it rapidly decomposes in RPMI cell culture medium with a half-life of 15 min. This decomposition process also generates reactive oxygen species (ROS). To identify the actual candidate(s) for the observed bioactivity of HA 14-1, we characterized the structures, quantified the amount, and evaluated the bioactivities of the decomposed products. We also used ROS scavengers to explore the function of ROS. From these studies, we established that none of the decomposition products could account for the bioactivity of HA 14-1. ROS generated during the decomposition process, however, are critical for the *in vitro* cytotoxicity and the apoptosis induced by HA 14-1. This study demonstrates that HA 14-1 is not stable under physiological conditions and that HA 14-1 can generate ROS through its decomposition, independent of Bcl-2 antagonism. Because of its intrinsic tendency to decompose and to generate ROS, caution should be taken in using HA 14-1 as a qualified antagonist against antiapoptotic Bcl-2 proteins.

Keywords: HA 14-1; Bcl-2; apoptosis; reactive oxygen species; decomposition

Introduction

Apoptosis is a highly regulated and energy-dependent cellular suicide process.[1] Bcl-2 protein family are crucial regulators of apoptosis.[2] Some Bcl-2 family proteins are antiapoptotic, such as Bcl-2, Bcl-X_L, and Bcl-w.[3,4] These antiapoptotic Bcl-2 proteins are often overexpressed in various malignancies, and such overexpression is one general mechanism via which cancer cells develop drug resistance against cancer therapies.[5–7] Antagonizing the antiapoptotic

* To whom correspondence should be addressed: Department of Medicinal Chemistry, College of Pharmacy, University of Minnesota, 8-101 WDH, 308 Harvard St. SE, Minneapolis MN 55455. Telephone: (612) 626-5675. Fax: (612) 624-0139. E-mail: xingx009@umn.edu.

[†] These authors contributed equally to this research.

(1) Thompson, C. B. Apoptosis in the pathogenesis and treatment of disease. *Science* **1995**, *267*, 1456–1462.

(2) Reed, J. C. Bcl-2 family proteins. *Oncogene* **1998**, *17*, 3225–3236.

(3) Adams, J. M.; Cory, S. Life-or-death decisions by the Bcl-2 protein family. *Trends Biochem. Sci.* **2001**, *26*, 61–66.

(4) Reed, J. C. Apoptosis-based therapies. *Nat. Rev. Drug Discovery* **2002**, *1*, 111–121.

10.1021/mp7000846 CCC: $37.00
Published on Web 09/18/2007

Bcl-2 proteins, therefore, can be a valuable strategy for overcoming drug resistance in cancer treatment. This concept has been proven by the preclinical and clinical results of Genasense, an antisense oligonucleotide against Bcl-2.[8] Currently, there are also quite a few small-molecule antagonists that are at various stages of development as anticancer agents.[9–18] Of these, ABT-737 is the most potent antagonist, which can disrupt the heterodimerization of antiapoptotic Bcl-2 proteins with proapoptotic Bcl-2 proteins and demonstrates *in vivo* anticancer activity.[15]

Ethyl-2-amino-6-bromo-4-(1-cyano-2-ethoxy-2-oxoethyl)-4*H*-chromene-3-carboxylate (HA 14-1) is one of the earliest reported small-molecule antagonists against antiapoptotic Bcl-2 proteins.[9] Recently, several studies showed that HA 14-1 could selectively eliminate tumor cells overexpressing Bcl-2 protein.[19–21] In the study by Dai et al.,[19] leukemia cells developed resistance to Imatinib over the course of treatment through the overexpression of Bcl-2. These Imatinib-resistant cells, however, were more sensitive to HA 14-1 than the parent leukemia cells. These studies underscore the potential of HA 14-1 in selectively targeting drug-resistant tumors. Moreover, many studies demonstrated that HA 14-1 sensitized cancer cells to a wide variety of cancer therapies (Table 1),[19,20,22–32] highlighting the promise of HA 14-1 as a chemosensitizer in the combination therapy for cancer treatment. Because of its great potential in cancer therapy and its proposed antagonism against antiapoptotic Bcl-2 proteins,

(5) Bouillet, P.; Cory, S.; Zhang, L. C.; Strasser, A.; Adams, J. M. Degenerative disorders caused by Bcl-2 deficiency prevented by loss of its BH3-only antagonist Bim. *Dev. Cell* **2001**, *1*, 645–653.

(6) Cory, S.; Huang, D. C.; Adams, J. M. The Bcl-2 family: Roles in cell survival and oncogenesis. *Oncogene* **2003**, *22*, 8590–8607.

(7) Genta Proportion of patients who at the time of diagnosis overexpress Bcl-2 relative to a normal cellular population. http://www.genta.com/genta/Products/bcl2.html. 2006.

(8) Kim, R.; Emi, M.; Tanabe, K.; Toge, T. Therapeutic potential of antisense Bcl-2 as a chemosensitizer for cancer therapy. *Cancer* **2004**, *101*, 2491–2502.

(9) Wang, J.; Liu, D.; Zhang, Z.; Shan, S.; Han, X.; Srinivasula, S. M.; Croce, C. M.; Alnemri, E. S.; Huang, Z. Structure-based discovery of an organic compound that binds Bcl-2 protein and induces apoptosis of tumor cells. *Proc. Natl. Acad. Sci. U.S.A.* **2000**, *97*, 7124–7129.

(10) Lugovskoy, A. A.; Degterev, A. I.; Fahmy, A. F.; Zhou, P.; Gross, J. D.; Yuan, J.; Wagner, G. A Novel Approach for Characterizing Protein Ligand Complexes: Molecular Basis for Specificity of Small-Molecule Bcl-2 Inhibitors. *J. Am. Chem. Soc.* **2002**, *124*, 1234–1240.

(11) Tzung, S.; Kim, K. M.; Basañez, G.; Giedt, C. D.; Simon, J.; Zimmerberg, J.; Zhang, K. Y. J.; Hockenbery, D. M. Antimycin A mimics a cell-death-inducing Bcl-2 homology domain 3. *Nat. Cell Biol.* **2001**, *3*, 183–191.

(12) Enyedy, I. J.; Ling, Y.; Nacro, K.; Tomita, Y.; Wu, X.; Cao, Y.; Guo, R.; Li, B.; Zhu, X.; Huang, Y.; Long, Y.; Roller, P. P.; Yang, D.; Wang, S. Discovery of Small-Molecule Inhibitors of Bcl-2 through Structure-Based Computer Screening. *J. Med. Chem.* **2001**, *44*, 4313–4324.

(13) Becattini, B.; Kitada, S.; Leone, M.; Monosov, E.; Chandler, S.; Zhai, D.; Kipps, T. J.; Reed, J. C.; Pellecchia, M. Rational Design and Real Time, In-Cell Detection of the Proapoptotic Activity of a Novel Compound Targeting Bcl-XL. *Chem. Biol.* **2004**, *11*, 389–395.

(14) Kitada, S.; Leone, M.; Sareth, S.; Zhai, D.; Reed, J. C.; Pellecchia, M. Discovery, Characterization, and Structure-Activity Relationships Studies of Proapoptotic Polyphenols Targeting B-Cell Lymphocyte/Leukemia-2 Proteins. *J. Med. Chem.* **2003**, *46*, 4259–4264.

(15) Oltersdorf, T.; Elmore, S. W.; Shoemaker, A. R.; Armstrong, R. C.; Augeri, D. J.; Belli, B. A.; Bruncko, M.; Deckwerth, T. L.; Dinges, J.; Hajduk, P. J.; Joseph, M. K.; Kitada, S.; Korsmeyer, S. J.; Kunzer, A. R.; Letai, A.; Li, C.; Mitten, M. J.; Nettesheim, D. J.; Ng, S.; Nimmer, P. M.; O'Connor, J. M.; Oleksijew, A.; Petros, A. M.; Reed, J. C.; Shen, W.; Tahir, S. K.; Thompson, C. B.; Tomaselli, K. J.; Wang, B.; Wendt, M. B.; Zhang, H.; Fesik, S. W.; Rosenberg, S. H. An inhibitor of Bcl-2 family proteins induces regression of solid tumours. *Nature* **2005**, *435*, 677–681.

(16) Petros, A. M.; Dinges, J.; Augeri, D. J.; Baumeister, S. A.; Betebenner, D. A.; Bures, M. G.; Elmore, S. W.; Hajduk, P. J.; Joseph, M. K.; Landis, S. K.; Nettesheim, D. G.; Rosenberg, S. H.; Shen, W.; Thomas, S.; Wang, X.; Zanze, I.; Zhang, H.; Fesik, S. W. Discovery of a Potent Inhibitor of the Antiapoptotic Protein Bcl-xL from NMR and Parallel Synthesis. *J. Med. Chem.* **2006**, *49*, 656–663.

(17) Tang, G.; Yang, C. Y.; Nikolovska-Coleska, Z.; Guo, J.; Qiu, S.; Wang, R.; Gao, W.; Wang, G.; Stuckey, J.; Krajewski, K.; Jiang, S.; Roller, P. P.; Wang, S. Pyrogallol-based molecules as potent inhibitors of the antiapoptotic Bcl-2 proteins. *J. Med. Chem.* **2007**, *50*, 1723–1726.

(18) Verhaegen, M.; Bauer, J. A.; Martin de la Vega, C.; Wang, G.; Wolter, K. G.; Brenner, J. C.; Nikolovska-Coleska, Z.; Bengtson, A.; Nair, R.; Elder, J. T.; Van Brocklin, M.; Carey, T. E.; Bradford, C. R.; Wang, S.; Soengas, M. S. A novel BH3 mimetic reveals a mitogen-activated protein kinase-dependent mechanism of melanoma cell death controlled by p53 and reactive oxygen species. *Cancer Res.* **2006**, *66*, 11348–11359.

(19) Dai, Y.; Rahmani, M.; Corey, S. J.; Dent, P.; Grant, S. A Bcr/Abl-independent, Lyn-dependent Form of Imatinib Mesylate (STI-571) Resistance Is Associated with Altered Expression of Bcl-2. *J. Biol. Chem.* **2004**, *279*, 34227–34239.

(20) Lickliter, J. D.; Wood, N. J.; Johnson, L.; McHugh, G.; Tan, J.; Wood, F.; Cox, J.; Wickham, N. W. HA14-1 selectively induces apoptosis in Bcl-2-overexpressing leukemia/lymphoma cells, and enhances cytarabine-induced cell death. *Leukemia* **2003**, *17*, 2074–2080.

(21) Su, Y.; Zhang, X.; Sinko, P. J. Exploration of drug-induced Bcl-2 overexpression for restoring normal apoptosis function: A promising new approach to the treatment of multidrug resistant cancer. *Cancer Lett.* **2007**, *253*, 115–123.

(22) Pei, X.; Dai, Y.; Grant, S. The proteasome inhibitor bortezomib promotes mitochondrial injury and apoptosis induced by the small molecule Bcl-2 inhibitor HA14-1 in multiple myeloma cells. *Leukemia* **2003**, *17*, 2036–2045.

(23) Hao, J.; Yu, M.; Liu, F.; Newland, A. C.; Jia, L. Bcl-2 Inhibitors Sensitize Tumor Necrosis Factor-Related Apoptosis-Inducing Ligand-Induced Apoptosis by Uncoupling of Mitochondrial Respiration in Human Leukemic CEM Cells. *Cancer Res.* **2004**, *64*, 3607–3616.

(24) Sinicrope, F. A.; Penington, R. C.; Tang, X. M. Tumor Necrosis Factor-Related Apoptosis-Inducing Ligand-Induced Apoptosis Is Inhibited by Bcl-2 but Restored by the Small Molecule Bcl-2 Inhibitor, HA 14-1, in Human Colon Cancer Cells. *Clin. Cancer Res.* **2004**, *10*, 8284–8292.

HA 14-1 is intensely investigated with 11 research articles published in 2007 already.[21,30,33–41]

However, several reports imply that HA 14-1 may not be stable and recommend the preparation of a fresh sample in DMSO for study.[37,42] Given its therapeutic potential and wide biological application, we investigated the stability of HA 14-1 in RPMI cell culture medium. We found that HA 14-1 rapidly loses its *in vitro* cytotoxicity through decomposition upon incubation in RPMI. We also studied the decomposition process of HA 14-1. Specifically, we characterized the decomposition products and studied their biological activities, establishing that the decomposed products could not account for the *in vitro* cytotoxicity of HA 14-1 and that they did not interact with antiapoptotic Bcl-2 proteins. HA 14-1 decomposition also generates ROS, which are cytotoxic and induce apoptosis *in vitro*. On the basis of these studies, we conclude that HA 14-1 is not a stable candidate for clinical development and antagonizing antiapoptotic Bcl-2 proteins is not the sole mechanism of action for HA 14-1.

Materials and Methods

Reagents. Ethyl-2-amino-6-bromo-4-(1-cyano-2-ethoxy-2-oxoethyl)-4*H*-chromene-3-carboxylate (HA 14-1) was synthesized in the laboratory by following the established procedures and characterized by NMR and mass spectrometry.[43] 5-Bromosalicylaldehyde, ethyl cyanoacetate, vitamin E, *N*-acetyl-L-cysteine (LNAC), and Trypan Blue were all purchased from Sigma (St. Louis, MO). H_2DCFDA was purchased from Molecular Probes (Eugene, OR).

Cell Culture. Jurkat cells were cultured in RPMI medium supplemented with 10% fetal bovine serum at 37 °C with 5% CO_2.

***In Vitro* Cytotoxicity Assay.** The *in vitro* cytotoxicity of the small molecules was assayed by determining the GI_{50} (the concentration of a small molecule required to inhibit cell growth by 50%) values. In brief, Jurkat cells were plated in a 96-well plate at the density of 1×10^4 cells/well. A series of 3-fold dilutions of the test compounds with 1% DMSO in the final cell medium was used for the cell treatment (cells treated with medium containing 1% DMSO

(25) Nimmanapalli, R.; O'Bryan, E.; Kuhn, D.; Yamaguchi, H.; Wang, H.; Bhalla, K. N. Regulation of 17-AAG-induced apoptosis: Role of Bcl-2, Bcl-xL, and Bax downstream of 17-AAG-mediated down-regulation of Akt, Raf-1, and Src kinases. *Blood* **2003**, *102*, 269–275.

(26) Pei, X.; Dai, Y.; Grant, S. The small-molecule Bcl-2 inhibitor HA14-1 interacts synergistically with flavopiridol to induce mitochondrial injury and apoptosis in human myeloma cells through a free radical-dependent and Jun NH2-terminal kinase-dependent mechanism. *Mol. Cancer Ther.* **2004**, *3*, 1513–1524.

(27) Skommer, J.; Wlodkowic, D.; Mättö, M.; Eray, M.; Pelkonen, J. HA14-1, a small molecule Bcl-2 antagonist, induces apoptosis and modulates action of selected anticancer drugs in follicular lymphoma B cells. *Leuk. Res.* **2006**, *20*, 322–331.

(28) Manero, F.; Gautier, F.; Gallenne, T.; Cauquil, N.; Grée, D.; Cartron, P.-F.; Geneste, O.; Grée, R.; Vallette, F. M.; Juin, P. The Small Organic Compound HA14-1 Prevents Bcl-2 Interaction with Bax to Sensitize Malignant Glioma Cells to Induction of Cell Death. *Cancer Res.* **2006**, *66*, 2757–2764.

(29) Niizuma, H.; Nakamura, Y.; Ozaki, T.; Nakanishi, H.; Ohira, M.; Isogai, E.; Kageyama, H.; Imaizumi, M.; Nakagawara, A. Bcl-2 is a key regulator for the retinoic acid-induced apoptotic cell death in neuroblastoma. *Oncogene* **2006**, *25*, 5046–5055.

(30) An, J.; Chervin, A. S.; Nie, A.; Ducoff, H. S.; Huang, Z. Overcoming the radioresistance of prostate cancer cells with a novel Bcl-2 inhibitor. *Oncogene* **2007**, *26*, 652–661.

(31) Sutter, A. P.; Maaser, K.; Grabowski, P.; Bradacs, G.; Vormbrock, K.; Höpfner, M.; Krahn, A.; Heine, B.; Stein, H.; Somasundaram, R.; Schuppan, D.; Zeitz, M.; Scherübl, H. Peripheral benzodiazepine receptor ligands induce apoptosis and cell cycle arrest in human hepatocellular carcinoma cells and enhance chemosensitivity to paclitaxel, docetaxel, doxorubicin and the Bcl-2 inhibitor HA14-1. *J. Hepatol.* **2004**, *41*, 799–807.

(32) Milella, M.; Estrov, Z.; Kornblau, S. M.; Carter, B. Z.; Konopleva, M.; Tari, A.; Schober, W. D.; Harris, D.; Leysath, C. E.; Lopez-Berestein, G.; Huang, Z.; Andreeff, M. Synergistic induction of apoptosis by simultaneous disruption of the Bcl-2 and MEK/MAPK pathways in acute myelogenous leukemia. *Blood* **2002**, *99*, 3461–3464.

(33) Oliver, L.; Mahe, B.; Gree, R.; Vallette, F. M.; Juin, P. HA14-1, a small molecule inhibitor of Bcl-2, bypasses chemoresistance in leukaemia cells. *Leuk. Res.* **2007**, *31*, 859–863.

(34) Lickliter, J. D.; Cox, J.; McCarron, J.; Martinex, N. R.; Schmidt, C. W.; Lin, H.; Nieda, M.; Nicol, A. J. Small-molecule Bcl-2 inhibitors sensitise tumor cells to immune-mediated destruction. *Br. J. Cancer* **2007**, *96*, 600–608.

(35) Witters, L. M.; Witkoski, A.; Planas-Silva, M. D.; Berger, M.; Viallet, J.; Lipton, A. Synergistic inhibition of breast cancer cell lines with a dual inhibitor of EGFR-HER-2/neu and a Bcl-2 inhibitor. *Oncol. Rep.* **2007**, *17*, 465–469.

(36) Franke, C.; Noldner, M.; Abdel-Kader, R.; Johson-Anuna, L. N.; Gibson Wood, W.; Muller, W. E.; Eckert, G. P. Bcl-2 upregulation and neuroprotection in guninea pig brain following chronic simvastatin treatment. *Neurobiol. Dis.* **2007**, *25*, 438–445.

(37) Wlodkowic, D. Skommer, J. Pelkonen, J. Brefeldin A triggers apoptosis associated with mitochondrial breach and enhances HA 14-1- and anti-Fas-mediated cell killing in follicular lymphoma cells. *Leuk. Res.* **2007**, XXX. (in press).

(38) Kessel, D.; Reiners, J. J., Jr. Initiation of apoptosis and autophagy by the Bcl-2 antagonist HA 14-1. *Cancer Lett.* **2007**, *249*, 294–299.

(39) Wlodkowic, D.; Skommer, J.; Pelkonen, J. Towards an understanding of apoptosis detection by SYTO dyes. *Cytometry, Part A* **2007**, *71*, 61–72.

(40) Nsoure Obame, F. Zini, R. Souktani, R. Berdeaux, A. Morin, D. Peripheral Benzodiazepine Receptor-Induced Myocardial Protection is Mediated by Inhibition of Mitochondrial Membrane Permeabilization. *J. Pharmacol. Exp. Ther.* **2007**, XXX. (in press).

(41) Schwartz, P. S.; Manion, M. K.; Emerson, C. B.; Fry, J. S.; Schulz, C. M.; Sweet, I. R.; Hockenbery, D. M. 2-Methoxy antimycin reveals a unique mechanism for Bcl-xL inhibition. *Mol. Cancer Ther.* **2007**, *6*, 2073–2080.

(42) An, J.; Chen, Y.; Huang, Z. Critical Upstream Signals of Cytochrome c Release Induced by a Novel Bcl-2 Inhibitor. *J. Biol. Chem.* **2004**, *279*, 19133–19140.

(43) Doshi, J. M.; Tian, D.; Xing, C. Structure-activity relationship studies of ethyl 2-amino-6-bromo-4-(1-cyano-2-ethoxy-2-oxoethyl)-4H-chromene-3-carboxylate (HA 14-1), an antagonist for antiapoptotic Bcl-2 proteins to overcome drug resistance in cancer. *J. Med. Chem.* **2006**, *49*, 7731–7739.

Table 1. Reported Synergism of HA 14-1 with Respect to Various Cancer Therapies in Different Tumor Types

drug	mechanism of action	course of treatment	cell type	Bcl-2 level
etoposide[19]	TopoII inhibitor	simultaneous	CML	overexpressing
cytarabine[20]	antimetabolite	cytarabine pretreat	AML/CML	overexpressing
bortezomib[22]	proteasome inhibitor	bortezomib pretreat	myeloma	endogenous
TRAIL[23]	death ligand	HA 14-1 pretreat	leukemia	overexpressing
TRAIL[24]	death ligand	simultaneous	colon	endogenous
17-AAG[25]	HSP-90 inhibitor	simultaneous	HL-60	overexpressing
flavopiridol[26]	CDK inhibitor	simultaneous or HA 14-1 pretreat	myeloma	endogenous
flavopiridol[26]	CDK inhibitor	flavopiridal pretreat	myeloma	endogenous
dexamethasone[27]	apoptotic inducer	simultaneous/HA 14–1 pretreat	follicular lymphoma	overexpressing
doxorubicin[27]	TopoII inhibitor	simultaneous/HA 14-1 pretreat	follicular lymphoma	overexpressing
radiation[28]	DNA damage	HA 14-1 pretreat	glioblastoma	overexpressing
etoposide[28]	TopoII inhibitor	HA 14-1 pretreat	glioblastoma	overexpressing
retinoic acid[29]	differentiating agent	simultaneous	neuroblastoma	endogenous
radiation[30]	DNA damage	HA 14-1 pretreat	prostate	endogenous
FGIN-1–27[31]	Peripheral benzodiazepine receptor ligand	simultaneous	liver	endogenous
PD185352[32]	MEK/MAKR inhibitor	simultaneous	AML	endogenous

served as a control). For stability studies, an identical set of the test compounds was incubated at 37 °C for the specified time period and then were used along with freshly prepared samples to treat Jurkat cells. After a 24 h treatment, the relative cell viability in each well was determined by using CellTiter-Blue Cell Viability Assay Kit [a fluorescence assay that measures the degree of reduction of a dye (resazurin) into a fluorescent end product (resorufin) by metabolically active cells – viable cells] (Promega). The GI_{50} of each candidate was determined by fitting the relative viability of the cells to the drug concentration by using a dose–response model in GraphPad. For the protective effect of LNAC and vitamin E against HA 14-1 *in vitro*, a long-term colony assay was used. Briefly, Jurkat cells were treated with HA 14-1, LNAC, vitamin E, or their combination for 24 h. The cells were then cultured in fresh RPMI medium for an additional 5 days. The amount of living cells was counted with Trypan Blue staining.

Rate of Decomposition of HA 14-1 in RPMI. A stock solution of HA 14-1 in dimethyl sulfoxide (20 mM) was added to prewarmed RPMI cell culture medium to obtain a final HA 14-1 concentration of 200 μM. Such a solution was incubated at 37 °C for specified times (0, 5, 15, 30, 60, 180, and 1440 min). The solution was mixed with an equal volume of a 4-bromophenol solution (internal standard, 200 μM) in methanol and analyzed by reversed-phase high-performance liquid chromatography (HPLC). HPLC was performed on a Beckman Coulter System Gold 126 solvent module and 168 detector. A Phenomenex Polar RP column (5 μm, 250 mm × 4.6 mm) was used for the analyses. The flow rate was 0.7 mL/min. Mobile phase A was water, while phase B was acetonitrile. The time program used for the analyses was as follows: 95% A from 0 to 5 min, 5 to 95% B from 5 to 35 min, 95% B from 35 to 40 min, and 5 to 95% A from 40 to 42 min). To determine whether ROS initiate or facilitate the decomposition of HA 14-1, similar experiments were carried out in the presence of 1.67 mM LNAC.

Characterization of Decomposition Products. A stock solution of HA 14-1 in deuterated dimethyl sulfoxide (50 mM, 400 μL) was added to prewarmed cell culture medium (40 mL) to produce a final HA 14-1 concentration of 500 μM. This solution was then incubated at 37 °C for 3 h. Following this, the solution was cooled and extracted with 3 × 25 mL of methylene chloride. The organic extracts were collected and concentrated to produce a d_6-DMSO residue. The d_6-DMSO residue was dissolved in $CDCl_3$ (600 μL) with benzene (45 mM) as the internal standard. Such a solution was analyzed by ^{1}H NMR. Characteristic peaks were used for structure determination and the quantification of various candidates. The aqueous fraction was mixed with an equal volume of a 4-bromophenol solution in methanol (200 μM). The mixture was analyzed by HPLC following the HPLC method detailed above.

Binding to Antiapoptotic Bcl-2 Proteins. The binding interactions of the decomposed products from HA 14-1 with Bcl-2, Bcl-X_L, and Bcl-w proteins were evaluated by following an established protocol.[43]

Cell-Free ROS Assay. Dichlorodihydrofluorescein, which can be oxidized by ROS to dichlorofluorescein, was prepared from H_2DCFDA by alkaline hydrolysis, according to the methods of Cathcart et al.[44] Briefly, 6.4 μL of 25 mM H_2DCFDA in DMSO was added to 32 μL of aqueous NaOH (100 mM), which was allowed to stand at room temperature for 30 min. Hydrolyte was then neutralized with 4 mL of PBS and kept on ice before use. Within 3 h of its preparation, 50 μL of the de-acetylated probe was transferred to each well in a 96-well plate, and 50 μL of the compound of interest in PBS with 2% DMSO was then added to each well. The formation of ROS was assessed kinetically by following the fluorescence intensity change with excitation at 485 nm and emission at 530 nm in a 96-well plate with a 100 μL

(44) Cathcart, R.; Schwiers, E.; Ames, B. N. Detection of picomole levels of hydroperoxides using a fluorescent dichlorofluorescein assay. *Anal. Biochem.* **1983**, *134*, 111–116.

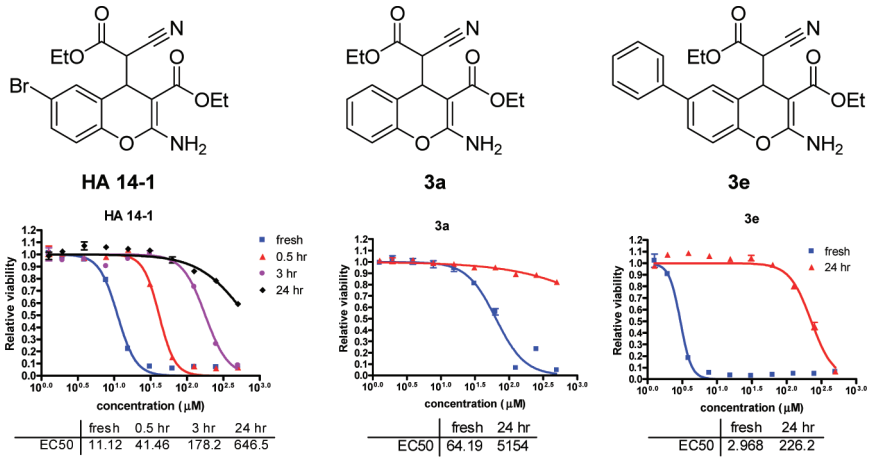

Figure 1. Loss of cytotoxicities of HA 14-1 and its analogues upon incubation in RPMI cell culture medium.

sample in each well. ROS intensity in each well was normalized to the vehicle-treated control.

Intracellular ROS Assay in Jurkat Cells. Jurkat cells were adjusted to a cell density of 8×10^5 cells/mL in PBS. Such a cell suspension (5 mL) was transferred in a 5 cm round Petri dish. To one cell sample was added 4 μL of 25 mM H_2DCFDA dye in DMSO; to another cell sample was added 4 μL of DMSO, and such cells served as a control. These cell samples were incubated at 37 °C for 30 min to allow intracellular de-esterification of H_2DCFDA to dichlorodihydrofluorescein. Such cell samples were collected by centrifugation, washed twice with PBS, and resuspended in PBS (3 mL). These cell samples (0.25 mL) were mixed with the compound of interest in PBS with 2% DMSO (0.25 mL). ROS generation was followed kinetically by following the fluorescence intensity change with excitation at 485 nm and emission at 530 nm in a 96-well plate with 100 μL of sample in each well. ROS intensity in each well was normalized to the vehicle-treated control.

Caspase-3/-7 Activation. An Apo-ONE Homogeneous Caspase-3/-7 Assay Kit from Promega was used to measure the caspase-3/-7 activity according to the manufacturer's instructions. Briefly, after the indicated drug treatment, Apo-ONE Caspase-3/-7 reagent (50 μL) was added to each well containing 50 μL of cell suspension (4×10^4 cells) in a 96-well plate. The suspension in the wells were mixed gently and incubated at 37 °C for 30–60 min. The activity of caspase-3/-7 was measured by following the fluorescence intensity with excitation at 485 nm and emission at 530 nm. The relative caspase-3/-7 activity in each well was normalized to that of the vehicle-treated control cell.

DNA Fragmentation Assay. DNA fragmentation was assessed with the Apoptotic DNA Ladder Extraction Kit from Biovision. Briefly, Jurkat cells (2.0×10^6) were treated with HA 14-1 (20 μM) or HA 14-1 (20 μM) and other agents at their specified concentrations for 4 h. Such cells were harvested and washed with PBS. The supernatant was removed by pipetting. The cell pellet was suspended in DNA Ladder Extraction Buffer (50 μL) and incubated at 23 °C for 10 s with gentle tapping. The mixture was centrifuged for 5 min at 1600*g*. The supernatant was transferred to a fresh tube. The cell pellet was extracted again with DNA Ladder Extraction Buffer (50 μL). The supernatants were combined, and enzyme A solution (5 μL) was added to it. The solution was mixed by gentle vortexing and incubated at 37 °C for 10 min. Enzyme B solution (5 μL) was then added to the mixture and further incubated overnight at 50 °C. An ammonium acetate solution (5 μL, provided with the kit) was added to the sample and mixed well. 2-Propanol (100 μL) was added, and the solution was mixed well and kept at −20 °C for 20 min. The DNA pellet was obtained by centrifugation of the 2-propanol suspension at 13000*g* for 10 min. The pellet was washed twice with cold 75% ethanol. The pellet was dried and resuspended in DNA suspension buffer (20 μL). Samples were loaded on to a 1.2% agarose gel containing 0.5 μg/mL ethidium bromide in both the gel and the running buffer. Electrophoresis was conducted at 50 V for 1 h. DNA was visualized with UV light and photographed.

Statistical Analysis. All biological experiments, including binding assays, *in vitro* cytotoxicity assays, caspase-3/-7 assays, and ROS assays, were performed at least twice with triplicates in each experiment. Representative results are depicted in this report. Data were analyzed and presented using GraphPad. Student's *t* test was applied for comparison between groups using GraphPad. Significance was set at $P < 0.05$.

Results and Discussion

HA 14-1 Stability. To quickly determine whether HA 14-1 was stable under physiological conditions, we first assayed the change in the cytotoxicity of HA 14-1 after it was incubated in cell culture medium. The rationale was that the incubated HA 14-1 solution should have the same cytotoxicity as the freshly prepared solution if HA 14-1 is stable in cell culture medium. Briefly, we prepared a series of HA 14-1 solutions of different concentrations in cell culture medium. Such solutions were incubated at 37 °C for varying periods of time (0, 0.5, 3, and 24 h). These HA 14-1 solutions were then evaluated for their *in vitro* cytotoxicity against Jurkat cells. As shown in Figure 1, a 0.5 h incubation of HA 14-1 in cell culture medium resulted in the loss of most

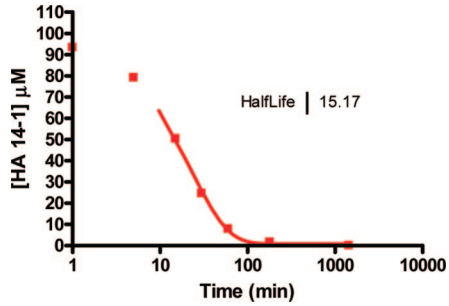

Figure 2. Half-life of HA 14-1 in RPMI cell culture medium, estimated by HPLC quantification of HA 14-1 preincubated in RPMI cell culture medium.

of its cytotoxicity (GI_{50} increased ~4-fold), and a 24 h incubation resulted in the total loss of cytotoxicity (GI_{50} increased ~60-fold). The rapid loss of cytotoxicity suggests that HA 14-1 is not stable in RPMI medium. Two HA 14-1 analogues developed in this laboratory (**3a** and **3e**) also rapidly lost their cytotoxicities upon incubation in RPMI medium (Figure 1). The structural comparison of HA 14-1, **3a**, and **3e** suggests that the instability of HA 14-1 may derive from its highly functionalized chromene ring. The half-life of HA 14-1 in RPMI was determined by HPLC quantification of HA 14-1 in the preincubated RPMI samples (Figure 2, HPLC spectra with HA 14-1 quantification in the Supporting Information). HA 14-1 has a half-life of ~15 min, confirming that HA 14-1 rapidly decomposes in RPMI medium.

The fact that HA 14-1 rapidly decomposes and loses *in vitro* cytotoxicity raised the question of whether HA 14-1 is the bioactive candidate or a decomposed intermediate may induce the observed cytotoxicity. It is critical to understand how HA 14-1 decomposes as well, which can guide the development of stable analogues of HA 14-1.

Characterization of the Decomposition Products of HA 14-1. To define the decomposition pathway of HA 14-1 and to identify the exact candidate(s) responsible for the observed *in vitro* cytotoxicity, we next characterized the decomposition products of HA 14-1, including the structural determination, the yield quantification, and the bioactivity evaluation. Specifically, following a 3 h incubation of HA 14-1 in cell culture medium at 37 °C, the HA 14-1 solution was extracted with methylene chloride. The organic extract was dried, and the residue in the organic extract was analyzed by NMR. The identifiable candidates were quantified by NMR with benzene as the internal standard. Four compounds were identified in the organic extract (Figure 3), including HA 14-1 (3.95%), 5-bromosalicylaldehyde (2.46%), ethyl 6-bromo-2-oxo-2*H*-1-benzopyran-3-carboxylate (**A**) (28.27%), and ethyl cyanoacetate (74.16%) (NMR spectrum and quantification in the Supporting Information). The aqueous fraction was directly analyzed by HPLC and mass spectrometry. Three compounds were identified in the aqueous fraction (Figure 3), including **A** (0.75%), 5-bromosalicylaldehyde (0.39%), and 6-bromo-2-oxo-2*H*-1-benzopyran-3-carboxylate (**B**, 48.15%) (HPLC spectra and quantification in the Supporting Information).

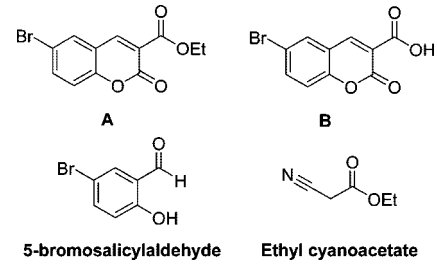

Figure 3. Structures of the four identified decomposition products of HA 14-1.

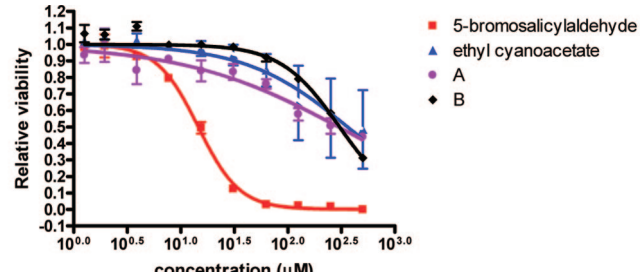

	5-bromosalicylaldehyde	ethyl cyanoacetate	A	B
EC50	14.59	361.3	296.6	304.8

Figure 4. *In vitro* cytotoxicities of the decomposed products of HA 14-1 against a Jurkat cell line.

The total mass balance of HA 14-1 from the organic extract and the aqueous fraction is 83.97% (the sum of HA 14-1, 5-bromosalicylaldehyde, **A**, and **B**). This relatively good mass balance suggests that we have identified most of the major candidates, if not all, generated from HA 14-1 decomposition. We also noticed that 5-bromosalicylaldehyde is not stable under the same conditions with an estimated half-life of ~170 min (Supporting Information). The potential loss of 5-bromosalicylaldehyde generated during the decomposition may account for some of the remaining mass balance. The identities of **A** and 5-bromosalicylaldehyde as decomposed products were verified by comparison with the authentic standards through NMR, HPLC, and mass spectrometry analyses. The identity of **B** as a decomposed product was verified by comparison with the authentic standard through HPLC and mass spectrometry analyses. The identity of ethyl cyanoacetate as one of the decomposed products was established by comparison with an authentic standard via NMR. Standard ethyl cyanoacetate and 5-bromosalicylaldehyde were purchased from Aldrich. Standards **A** and **B** were synthesized by following a reported alternate route.[45]

Subsequent biological evaluations of these decomposition products revealed that ethyl cyanoacetate, **A**, and **B** are much less cytotoxic *in vitro* than HA 14-1 [$GI_{50} \geq 300\ \mu M$ (Figure 4)]. Though 5-bromosalicylaldehyde is only slightly less cytotoxic than HA 14-1 ($GI_{50} = 14.6\ \mu M$), it is a minor decomposed product (<10%). These studies indicate that the decomposed products (even in combination) cannot account for the observed *in vitro* cytotoxicity of HA 14-1. Further-

(45) Bonsignore, L.; Cottiglia, F.; Maccioni, A. M.; Secci, D.; Lavagna, S. M. Synthesis of coumarin-3-O-acylisoureas by dicyclohexylcarbodiimide. *J. Heterocycl. Chem.* **1995**, *32*, 573–577.

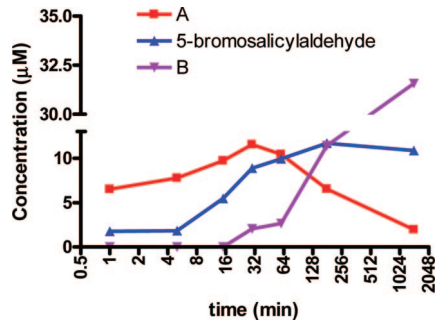

Figure 5. Time course abundance of **A**, **B**, and 5-bromosalicylaldehyde during HA 14-1 decomposition in RPMI cell culture medium.

more, none of these decomposed candidates with a concentration of up to 1 mM showed any binding interactions with antiapoptotic Bcl-2 proteins (data not shown).

Time Course Generation of the Decomposed Products. To deepen our understanding of the mechanism of the decomposition process, we used HPLC to characterize the time course generation of the decomposed products by HA 14-1 (Figure 5). It was found that both **A** and 5-bromosalicylaldehyde were detected immediately after HA 14-1 was mixed in RPMI medium, suggesting that they may be generated through two different pathways. **B** was not detected until HA 14-1 was mixed in RPMI for 30 min. Interestingly, we observed bell-shaped abundances of **A** and 5-bromosalicylaldehyde during the decomposition course, suggesting that **A** and 5-bromosalicylaldehyde further decompose. We also observed that as the abundance of **A** decreased, the abundance of **B** increased. On the basis of the fact that **A** decomposes, the late formation of **B**, and their structural differences, we propose that **A** hydrolyzes to form **B**. This hypothesis was further supported by the formation of **B** from pure **A** incubated in RPMI medium (Supporting Information). Of note, no 5-bromosalicylaldehyde was formed from **A** upon incubation in RPMI, establishing that 5-bromosalicylaldehyde generated during HA 14-1 decomposition is not derived from **A**. We, therefore, propose that HA 14-1 may decompose to generate **A** and 5-bromosalicylaldehyde through two independent pathways. In both pathways, ethyl cyanoacetate may be generated. **A** decomposes to generate **B** through hydrolysis. **B** seems to be stable in RPMI medium as incubation of pure **B** in RPMI medium resulted in no loss of **B** and no observable new product (Supporting Information). 5-Bromosalicylaldehyde further decomposes to unknown products as a 60 min incubation of pure 5-bromosalicylaldehyde in RPMI medium resulted in a 21% loss with no observable product detected (Supporting Information; the half-life of 5-bromosalicylaldehyde is estimated to be ~170 min). The loss of 5-bromosalicylaldehyde may be due to its condensation with amino-containing biomolecules in the medium or its oxidation to 5-bromosalicylic acid, which could be too hydrophilic to be separated from the solvent peak under our HPLC conditions.

Generation of ROS from HA 14-1 Decomposition. Several studies of HA 14-1 have revealed the generation of ROS in cancer cells when they were treated with HA 14-1, and such ROS have been shown to be responsible, at least in part, for the cytotoxicity and apoptosis induced by HA 14-1.[22,23,26,42] It remained to be determined how HA 14-1 treatment could lead to ROS generation, whether HA 14-1 generates ROS through its antagonism against antiapoptotic Bcl-2 proteins or through other mechanisms.

As we established that HA 14-1 could rapidly decompose in RPMI medium, we explored whether HA 14-1 could directly generate ROS through its decomposition, independent of its antagonism against antiapoptotic Bcl-2 proteins. We, therefore, evaluated ROS generation by HA 14-1 in cell-free PBS and in PBS with Jurkat cells (RPMI medium was not used in this study because of the high background interference of RPMI medium with ROS detection). Even in the cell-free PBS, HA 14-1 rapidly generated ROS (Figure 6A). The amount of ROS detected in cell-free PBS was higher than that detected in PBS with Jurkat cells (Figure 6B). The different ROS intensities in these two systems can be due to the accessibility of dichlorodihydrofluorescein to ROS. In the PBS system with Jurkat cells, dichlorodihydrofluorescein was preloaded in the cells and should only detect the intracellular ROS, which could be less abundant than the extracellular ROS. In cell-free PBS, HA 14-1 also induced ROS generation in a dose-dependent manner (Figure 6C), further supporting the idea that the observed ROS are generated from HA 14-1. The ability of HA 14-1 to generate ROS under cell-free conditions suggests that the ROS observed *in vitro* may not be derived from the antagonism of HA 14-1 against Bcl-2 proteins. Our results, however, cannot exclude the possibility that HA 14-1 may still be able to generate ROS through its interaction with cells. The two unstable analogues of HA 14-1 (**3a** and **3e**) also rapidly induce ROS generation in cell-free PBS (Figure 6D).

As HA 14-1 can decompose to form four products, ROS detected in cell-free PBS could be generated directly from any of the decomposed products of HA 14-1. It is also possible that ROS are generated during the decomposition process. To differentiate these two potential sources, we evaluated the decomposed products of HA 14-1 for their abilities to induce ROS generation under the same conditions. As shown in Figure 7A, none of the decomposed products generated ROS, even when they were combined together (not shown). Preincubated HA 14-1 (30 min) also failed to generate any ROS. These results overall suggest that HA 14-1 generates ROS directly during its decomposition process.

It is also interesting to determine whether ROS may facilitate the decomposition of HA 14-1 through a chain reaction as superoxide does for the oxidation of hydroquinone.[46,47] To address this possibility, we evaluated the stability of HA 14-1 in RPMI with ROS scavenged by LNAC (1.67 mM, based on the optimization detailed in the next section). As shown in Figure 7B, LNAC treatment had no major effect to the stability of HA 14-1 (half-life of 15.8 min compared to that of 15.2 min without LNAC treatment).

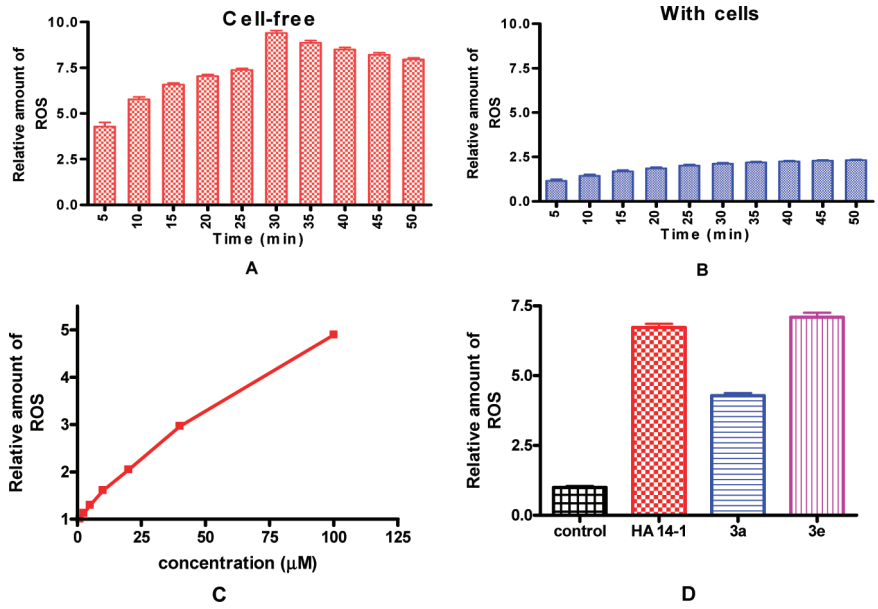

Figure 6. (A) Time-dependent generation of ROS by HA 14-1 (20 μM) treatment in PBS without cells. (B) Time-dependent intracellular generation of ROS by HA 14-1 (20 μM) treatment in Jurkat cells in PBS. (C) Dose–response ROS generation by HA 14-1 treatment in PBS without cells (30 min). (D) Generation of ROS by HA 14-1 and its analogues via **3a** and **3e** treatment at 20 μM in PBS without cells (30 min).

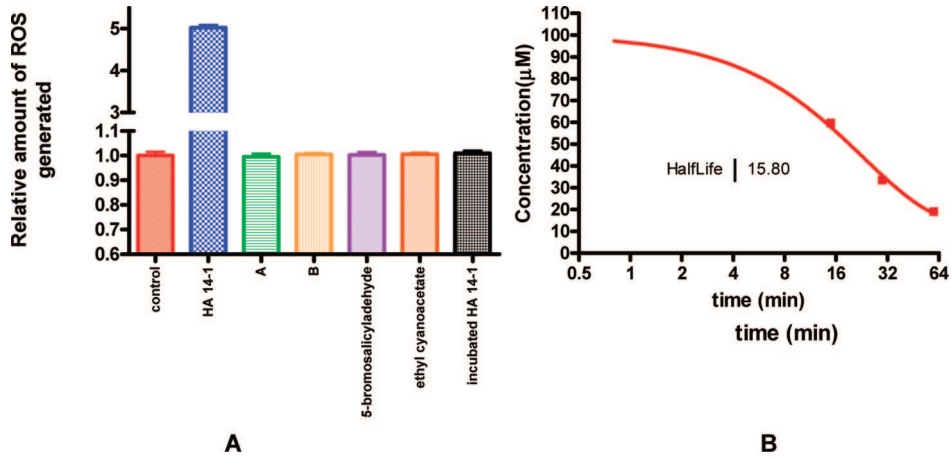

Figure 7. Source of ROS and its function in HA 14-1 decomposition. (A) Amount of ROS generated by fresh HA 14-1, the decomposed products of HA 14-1, and the preincubated HA 14-1 at 20 μM (30 min in PBS). (B) Half-life of HA 14-1 in RPMI in the presence of LNAC (1.67 mM).

This result suggests that ROS do not dramatically affect the decomposition of HA 14-1 under the conditions evaluated.

The Functions of ROS in HA 14-1 Induced Cytotoxicity and Apoptosis. We next explored the functions of ROS in the cytotoxicity and apoptosis induced by HA 14-1 *in vitro* by using ROS scavengers (LNAC and vitamin E). The optimal concentrations of LNAC and vitamin E used in our studies were determined by evaluating their efficacy in trapping ROS and their intrinsic toxicity. It was found that the most effective concentration of vitamin E to scavenge ROS was 200 μM (Supporting Information). Even at this concentration, vitamin E could only partially trap the ROS generated by HA 14-1, and it had a profound intrinsic toxicity with respect to Jurkat cells (Figure 8). These results suggest that vitamin E is not an optimal ROS scavenger under our experimental conditions. LNAC (1.67 mM), on the other hand, could scavenge the ROS generated by HA 14-1 to lower than the background level and induced no toxicity with respect to Jurkat cells at that concentration (Figure 8). We, therefore, used LNAC (1.67 mM) as the ROS scavenger to

(46) Munday, R. Autoxidation of naphthohydroquinones: Effects of metals, chelating agents, and superoxide dismutase. *Free Radical Biol. Med.* **1997**, *22*, 689–695.

(47) Ollinger, K.; Buffinton, G. D.; Ernster, L.; Cadenas, E. Effect of superoxide dismutase on the autoxidation of substituted hydro- and semi-naphthoquinones. *Chem.-Biol. Interact.* **1990**, *73*, 53–76.

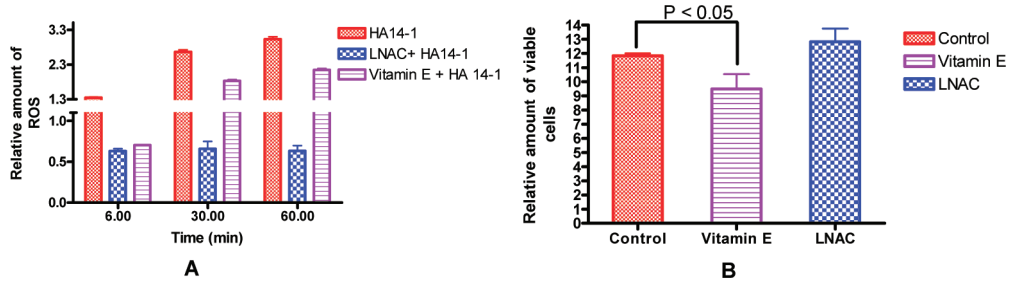

Figure 8. Optimization of the conditions for ROS scavengers. (A) Efficacy of LNAC (1.67 mM) and vitamin E (200 μM) in trapping ROS generated by HA 14-1 treatment (20 μM). (B) Toxicity of LNAC (1.67 mM) and vitamin E (200 μM) against Jurkat cells.

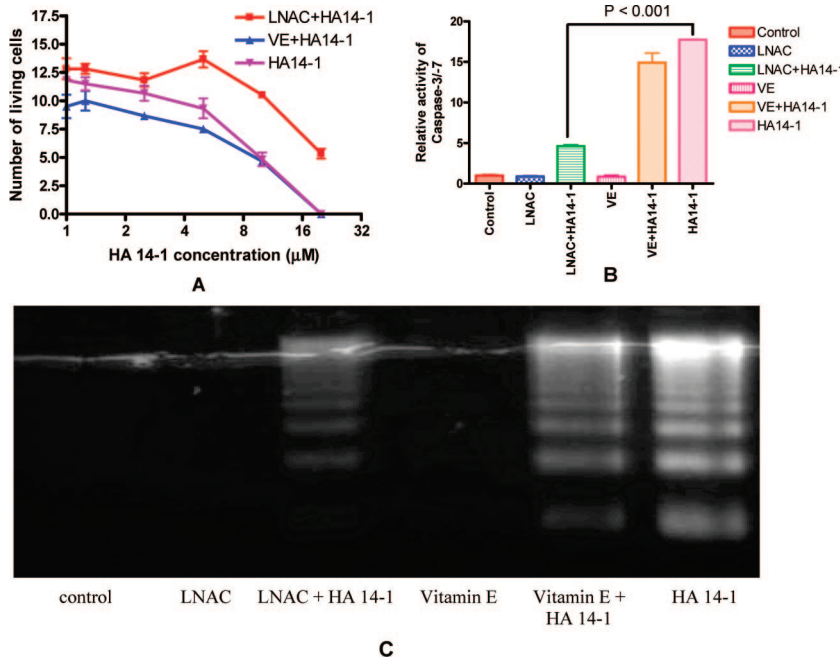

Figure 9. Protective effect of LNAC and vitamin E on Jurkat cells upon HA 14-1 treatment. (A) Cytotoxicity of HA 14-1 to Jurkat cells and the protective effect of LNAC and vitamin E. (B and C) Inhibitory effect of LNAC and vitamin E to apoptosis induced by HA 14-1 treatment in Jurkat cells: (B) activities of caspase-3/-7 and (C) DNA fragmentation.

Scheme 1. Proposed Major Decomposition Pathway of HA 14-1 in RPMI Cell Culture Medium

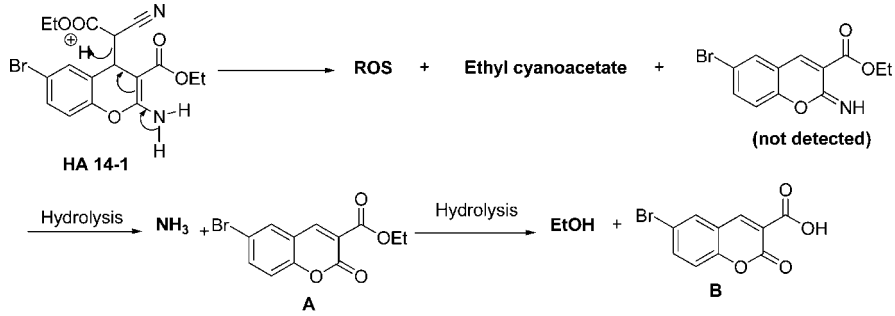

explore the function of ROS in the cytotoxicity and apoptosis induced by HA 14-1.

As shown in Figure 9A, 1.67 mM LNAC greatly reduced the toxicity induced by HA 14-1, especially at concentrations of 5, 10, and 20 μM. However, LNAC treatment could not completely mitigate the toxicity induced by HA 14-1 (10 and 20 μM). The partial protection by LNAC suggests that HA 14-1 may induce toxicity through mechanism(s) other than ROS, which could be related to its antagonism against antiapoptotic Bcl-2 proteins or the toxic activity of the decomposed products. LNAC treatment also greatly decreased the activity of caspase-3/-7 and DNA fragmentation induced by HA 14-1 (Figure 9B,C), supporting the possibility that ROS are critical for HA 14-1-induced apoptosis. Vitamin E, on the other hand, cannot induce much protection against the toxicity and apoptosis induced by HA 14-1 treatment. The lack of protection by vitamin E and its weak capability of scavenging ROS further support the fact that HA 14-1-

induced ROS are the major cytotoxic species for the *in vitro* activity of HA 14-1.

Decomposition Pathway of HA 14-1. On the basis of the decomposition products, their time course abundance, the decomposition profiles of **A** and 5-bromosalicylaldehyde, and the generation of ROS in the decomposition process and their effect on decomposition, we proposed the following possible decomposition pathway for HA 14-1 (Scheme 1). HA 14-1 can eliminate ethyl cyanoacetate to generate an undetected imine intermediate, which hydrolyzes to form **A**. **A** further hydrolyzes to form **B**. 5-Bromosalicylaldehyde may be generated from the decomposition of the imine intermediate or directly from HA 14-1, but not from **A** or **B**. Reactive oxygen species are also generated from HA 14-1 decomposition. Though our current studies cannot define the mechanism for their generation, we speculate that ROS may be generated during the formation of 5-bromosalicylaldehyde.

Conclusion

HA 14-1 has been widely used as an antagonist against antiapoptotic Bcl-2 proteins. In this report, we established that HA 14-1 rapidly decomposes with a half-life of 15 min in RPMI cell culture medium at 37 °C. We also identified the major decomposed products and established that none of them interact with antiapoptotic Bcl-2 proteins and none of them can account for the *in vitro* activities of HA 14-1. More importantly, we observed that HA 14-1, in a manner independent of its antagonism against antiapoptotic Bcl-2 proteins, can induce ROS generation directly through its decomposition process. ROS generated by HA 14-1 are in fact the major species responsible for the *in vitro* cytotoxicity and the apoptotic induction by HA 14-1.

In conclusion, our current studies demonstrate that HA 14-1 is not a qualified small-molecule antagonist against antiapoptotic Bcl-2 proteins. A decomposition pathway was proposed, which has guided us in successfully developing a stable analogue of HA 14-1, sHA 14-1, which is currently under investigation.

Acknowledgment. We are grateful to the University of Minnesota for funding. We also thank Dr. Carston R. Wagner and the reviewers for invaluable discussion and recommendations.

Supporting Information Available: HPLC and NMR spectra with quantification of the decomposition products of HA 14-1 in RPMI medium and abilities of LNAC and vitamin E to scavenge ROS induced by HA 14-1 (20 μM) in cell-free PBS and their intrinsic toxicity against Jurkat cells. This material is available free of charge via the Internet at http://pubs.acs.org.

MP7000846